

Electronic structure study using density functional theory in organic dendrimers

Rocio-Margarita Gutiérrez-Pérez ·
Norma Flores-Holguín · Daniel Glossmann-Mitnik ·
Luz-Maria Rodriguez-Valdez

Received: 21 July 2010 / Accepted: 31 October 2010 / Published online: 1 December 2010
© Springer-Verlag 2010

Abstract The electronic and structural properties of pyrrolic ring derivatives were studied using density functional theory (DFT) in terms of their application as organic semiconductor materials in photovoltaic devices. The B3LYP hybrid functional in combination with Pople type 6-31G(d) basis set with a polarization function was used in order to determine the optimized geometries and the electronic properties of the ground state, while transition energies and excited state properties were obtained from time-dependent (TD)-DFT with B3LYP/6-31G(d) calculation. The investigation of pyrrolic derivatives formed by the arrangement of several monomeric units revealed that three-dimensional (3D) conjugated architectures in which the combination of a triphenylamine (TPA) core with π -conjugated rings attached to the core, present the best geometric and electronic characteristics for use as an organic semiconductor material. The highest occupied molecular orbital (HOMO) – lowest unoccupied molecular orbital (LUMO) energy gap was decreased in 3D-structures that extend the absorption spectrum toward longer wavelengths, revealing a feasible intramolecular charge transfer process in these systems. All calculations in this work were performed using the Gaussian 03 W software package.

Keywords Density functional theory · Organic photovoltaics · Dendrimers and semiconductors

R.-M. Gutiérrez-Pérez · L.-M. Rodriguez-Valdez
Facultad de Ciencias Químicas,
Universidad Autónoma de Chihuahua,
Chihuahua, Chihuahua, México

N. Flores-Holguín (✉) · D. Glossmann-Mitnik
Química de Materiales,
Centro de Investigación en Materiales Avanzados,
Chihuahua, Chihuahua, México
e-mail: norma.flores@cimav.edu.mx

Introduction

Devices based on organic semiconductors are presently highly competitive for applications in electricity generation. In particular, organic solar cell research has achieved dramatic improvements in recent years, currently yielding efficiencies of around 5% [1]. The semiconducting properties of organic π -conjugated materials are an important area of research into easy and low-cost processing techniques to provide functionality and a large variety of applications such as organic light-emitting diodes (OLEDs) [2], organic photovoltaic (OPVs) [3], organic field-effect transistors (OFETs) [4, 5] and sensory materials [6, 7]. Such organic semiconductors include conjugated polymers and small molecular weight conjugated systems based largely on carbon and hydrogen, with small amounts of oxygen, nitrogen and sulfur in some materials [8].

One type of conjugated oligomer consists of well defined structures, named dendrimers, comprised of dendrons attached to a central core, which provide high processibility for applications in photovoltaic devices. These are three-dimensional (3D) man-made molecules produced by an unusual synthetic route that incorporates repetitive branching sequences to create a unique novel architecture with specific properties (electronic, optical, opto-electronic, magnetic, chemical, or biological) [9]. The dendrimers provide an excellent material for organic electronics [10]. Mitchell and co-workers [11] synthesized a series of first-generation thiophene-bridge dendrimers, and found that the electronic and optical band gaps decreased with increasing bridging of conjugated monomeric units; organic molecules derived from triphenylamine (TPA) have also been widely investigated [12]. The no-planarity in these types of molecules (TPA derivatives) and combinations with π -conjugated systems could improve charge-transport

properties. Such molecular arrangements have been reported previously by Nishimura et al. [13] and Ohishi and co-workers [14]. Theoretical studies that can help improve our understanding of structure-property relationships by systematically comparing theoretical description and electronic properties have also been published [15]. Suprtiz et al. [16] used a stochastic model to describe excitation transport in highly branched dendrimers in order to investigate the influence of an energy capturing reaction center on such transport.

Systems involving oligomers, dendrimers and π -conjugated polymers inherently possess a large number of possible combinations; in this sense, before starting a chemical synthesis it is convenient to check the molecular arrangement using quantum-chemical methods. For example, Beenken [17] performed a theoretical study of the photo-induced charge transfer in organic materials, increasing the number of monomeric units to provide sufficient optical absorption. Yang et al. [18] used applied quantum-chemical techniques to investigate the structural, electronic and optical properties of a series of thiophene oligomers, and showed that as the conjugation lengths increase the energy gaps decrease, and thus the absorption spectra exhibit bathochromic shift.

Here, we report the structural and electronic properties of some pyrrolic derivatives of TPA dendrimers analyzed by theoretical methods and UV-vis absorption spectroscopy. The frontier energy behaviors of these compounds were also studied in order to investigate their potentiality in photovoltaic conversion. The compounds targeted in this study have a number of desirable characteristics related to their use in organic photovoltaics and OLEDs: (1) they contain pyrrole groups with molecular parameters similar to the thiophene derivatives that have been shown to be useful as molecular nanostructured materials; (2) π -conjugated derivatives are generally efficient fluorophores and, as such, are useful for the fabrication of nanobiosensors; (3) they can be used as attractive building blocks for organic molecular materials [19].

Theory and computational details

There is much debate about which electronic structural method is best to model or describe the electronic properties in π -conjugated systems correctly [20]; however, it was recently shown that the hybrid density functional B3LYP [21] level of theory, which is a hybrid Hartree-Fock density functional theory (HF-DFT) functional that combines Becke's three parameter exchange functional [22] with Lee-Yang-Parr's correlation functional [23] in combination with the 6-31G(d) [24] basis set with polarization functions, provides good results for structural and excited state electronic properties in short conjugated systems [25–27]. The application of a hybrid-

functional is recommended for studies of charge transfer phenomena, especially where the exchange interaction is an important aspect to evaluate [17, 22]. Equilibrium geometries in ground state calculations were done using the B3LYP functional and 6-31G(d) basis set. The analytical frequency calculations were carried out for each stationary structure to verify if it is a minimum or a saddle point of first order. Excited state calculations in all pyrrolic derivatives were obtained by time-dependent (TD)-DFT [28–30] using the same hybrid functional and basis set as for the ground state calculations by DFT. It has been reported that TD-DFT is not a good method for calculate π - π^* electronic transitions; however, our results lead to adequate description of these properties in excited state as reported in previous works with similar molecular systems [17, 25–27]. All computational studies were performed with the Gaussian 03 W simulation program [31].

Results and discussion

Geometry optimizations in the ground state

Figure 1 shows the monomeric units of four pyrrolic ring structures that form the basic construction units for the systems analyzed here: monomer 1 (4-metoxiphenyl)-[4-(4-metoxiphenyl)-1H-pyrrole-3-yl]-metanone; monomer 2 (4-nitrophenyl)-(4-phenyl-1H-pyrrole-3-yl)-metanone; monomer 3 [4-(4-nitrophenyl)-1H-pyrrole-3-yl]-[phenyl] metanone; and monomer 4 [4-(4-metoxiphenyl)-1H-pyrrole-3-yl] (phenyl) metanone. Figure 2 shows the sketch map of dimers 1-1A and 1-1B (formed with two units of monomer 1 in different arrangements), as well as the trimers 2-2-2 (created with three units of monomer 2), 3-3-3 and 4-4-4 (three monomeric units of monomers 3 and 4, respectively). Geometrical optimization calculations were performed with B3LYP/6-31G(d) level of theory for each of the proposed systems in the ground state. The results show that the 2-2-2, 3-3-3 and 4-4-4 molecules present star-shaped structures known as dendrimers, with 2-2-2 and 3-3-3 having a central TPA core, thus these systems could be classified as a TPA-based compounds. This arrangement can influence the absorption of incident sunlight—an important characteristic for the construction of organic solar cells. Optimized geometries are depicted in Fig. 3.

HOMO–LUMO energy gap

The energy calculation of the frontier orbitals: HOMO (highest occupied molecular orbital) and LUMO (lowest unoccupied molecular orbital), as well as the HOMO–LUMO energy gap (ΔE_{gap}), are very significant properties that can aid analysis of

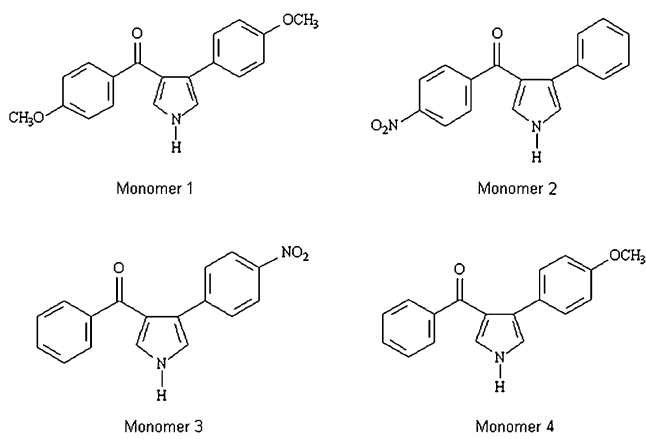


Fig. 1 Monomeric basic units of pyrrolic rings: monomer 1 [4-(4-methoxiphenyl)-[4-(4-methoxiphenyl)-1H-pyrrole-3-yl]-metanone; monomer 2 (4-nitrophenyl)-4-phenyl-1H-pyrrole-3-yl]-metanone; monomer 3 [4-(4-nitrophenyl)-1H-pyrrole-3-yl]-phenyl metanone; and monomer 4 [4-(4-methoxiphenyl)-1H-pyrrole-3-yl] (phenyl) metanone

the electronic behavior of these materials. The energy gap is considered as the energetic difference between the valence and conducting band, where, for organic materials, the HOMO is considered the valence band and the LUMO corresponds to the conducting band. This energy gap provides a reasonable indication of the excitation properties of these systems; thus, the smaller the energy gap, the bigger the excitation capability of material. Table 1 presents the values obtained for HOMO, LUMO and the HOMO–LUMO energy gap for all systems.

The energy gap calculation, $\Delta E_{\text{gap}} = (E_{\text{LUMO}} - E_{\text{HOMO}})$, in the ground state obtained with DFT B3LYP/6-31G(d) revealed an important difference in the proposed molecular arrangements, the energy gap results being in the order:

$$1 - 1\text{A} > 4 - 4 - 4 > 2 - 2 - 2 > 1 - 1\text{B} > 3 - 3 - 3$$

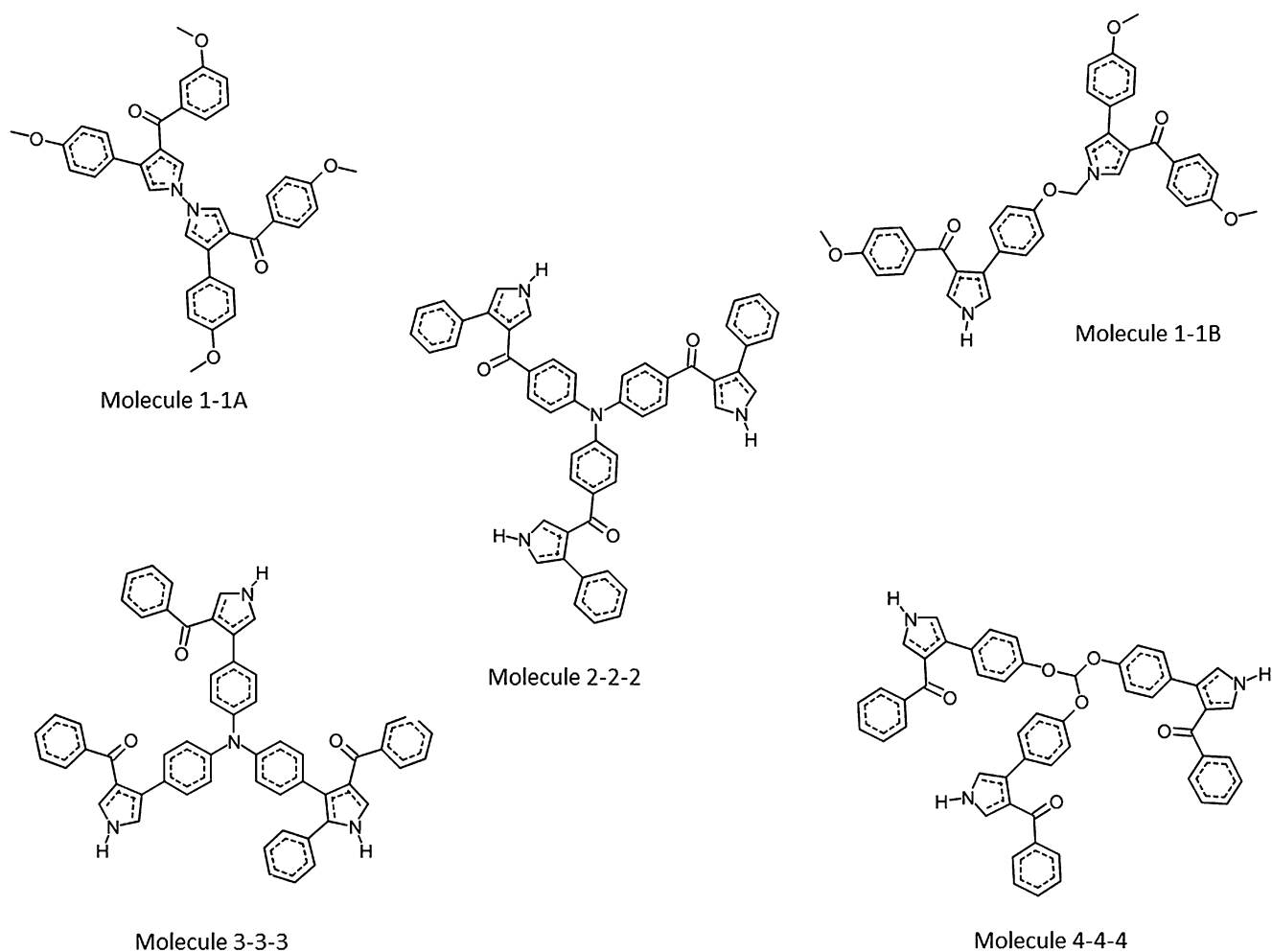


Fig. 2 Molecular structures of pyrrolic derivatives. Dimers 1-1A and 1-1B are formed from two units of monomer 1 in different arrangements, trimer 2-2-2 is created with three units of monomer 2, and trimers 3-3-3 and 4-4-4 from three monomeric units of monomers 3 and 4, respectively

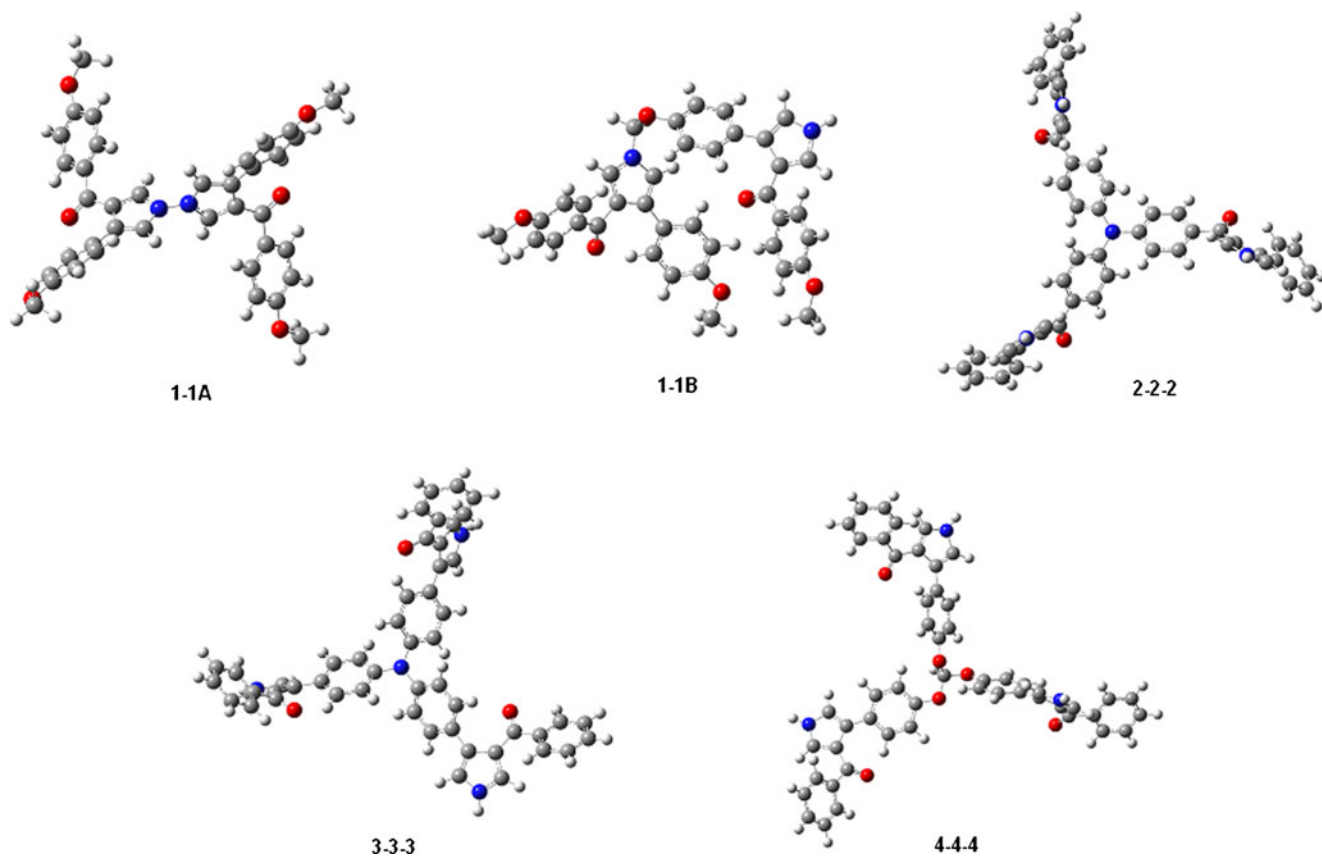


Fig. 3 Optimized geometries of the five structures shown in Fig. 2 using B3LYP/6-31G(d)

As can be seen in Table 1, the smallest HOMO–LUMO gap value (3.14 eV) was obtained for the 3-3-3 trimer—this value represents a considerable reduction (~ 1 eV) in the energy gap for the analyzed systems. As mentioned above, and from the results obtained, the 3-3-3 architecture thus represents the material most capable of excitation by incident sunlight with a reduced energy gap, which contributes to the performance of semiconductor materials.

Ultraviolet spectrum calculations

The potential of organic semiconducting materials for photovoltaic conversion, as well as their electronic properties, can be analyzed by UV-Vis absorption and emission spectroscopy [32]. For organic semiconductors in the relaxed

ground state geometry with appropriate HOMO–LUMO energy gaps, the absorption process begins when the material absorbs a photon (vertical absorption) and an electron-hole pair (exciton) is created. This exciton energy is then converted to electricity by the correct addressing of electrons and holes to the different electrodes in a solar cell. We applied TD-DFT B3LYP/6-31G(d) to all the optimized geometries to obtain the UV spectrum and the electronic transitions of all the structures under study. Table 2 lists the maximum absorption wavelength (λ_{\max}) and vertical absorption energies (Ω_A); the energy corresponding to the maximum in the spectrum absorption bands (excitation energies) can be compared with the vertical transition energies (vertical absorption) [33]. According to these results, the 2-2-2 and 3-3-3 molecules present the lowest

Table 1 HOMO (highest occupied molecular orbital) – LUMO (lowest unoccupied molecular orbital) energy gap (ΔE_{gap}) obtained with the DFT B3LYP/6-31G(d) model chemistry

Molecule	HOMO (eV)	LUMO (eV)	$\Delta E_{\text{gap}} = E_{\text{LUMO}} - E_{\text{HOMO}}$ (eV)
1-1A	-5.43	-1.33	4.10
1-1B	-4.90	-1.17	3.72
2-2-2	-5.36	-1.56	3.80
3-3-3	-4.30	-1.16	3.14
4-4-4	-5.20	-1.26	3.93

Table 2 Electronic absorption values calculated with time-dependent density functional theory (TD-DFT) B3LYP/6-31G(d) model chemistry, maximum absorption wavelength (λ_{\max}) and vertical absorption energy (Ω_A)

Molecule	λ_{\max} (nm)	Ω_A (eV)
1-1A	281.76	4.40
1-1B	283.77	4.37
2-2-2	373.61	3.32
3-3-3	335.77	3.69
4-4-4	275.85	4.49

values for vertical absorption energy at 3.32 and 3.69 eV, respectively, meaning that lower energy is required to cause an electronic transition.

Figure 4 shows the UV spectra for each compound obtained with TD-DFT B3LYP/6-31 G(d). Analysis of these spectra highlights the mismatch of the absorption spectrum of these materials and the terrestrial solar spectrum [34], where the maximum is between 500 and 800 nm [35]. However, the best performance is seen with the 2-2-2 and 3-3-3 dendrimers, with the latter presenting a small band close to the solar spectrum range. The most important characteristic for efficient photon harvesting [36] is the maximum absorption wavelength (λ_{\max}) value; for these compounds, λ_{\max} is 373.61 y 335.77 nm, respectively, corresponding to a $\pi-\pi^*$ transition. The increase in the number of aromatic rings in the molecules expanded the π -conjugated system, where the 2-2-2 and 3-3-3 arrangements present a bathochromic displacement in the absorption band, which means that a lower level of energy is necessary to promote an electron from lowest to highest energy levels, this agree with previous theoretical [37] and

experimental [38] works. The π -electrons are more easily excitable and can pass toward the orbitals of higher energy. There is a general rule that summarizes the effects of conjugation in the UV absorption wavelength: compounds containing a greater number of conjugated double bonds absorb light at longer wavelengths [37].

On the other hand, although all the trimers (2-2-2, 3-3-3 and 4-4-4) present a 3D conjugated architecture with the same number of π -conjugated rings (see Fig. 3), the 4-4-4 molecule presents the lowest λ_{\max} (275.85 nm), with a HOMO–LUMO energy gap of approximately 3.93 eV (see Table 1); these values could indicate a weak capacity for electronic semiconducting properties.

An individual analysis of absorption spectra is reported in Fig. 5. It should be noted that all compounds present a maximum absorption band corresponding to $\pi-\pi^*$ transitions in a range of 275–373 nm, where the $\pi-\pi^*$ electronic transition character is due mainly to HOMO→LUMO transitions. A previous experimental study [38] on similar 3D materials has shown that the emergence of a new transition or second band could be assigned to an intramolecular charge transfer (ICT) in the system. Comparison of the spectra of compounds 1-1A, 3-3-3 and 4-4-4 could indicate the appearance of a new transition or ICT band with an increment in intensity.

Localization of front molecular orbitals

The theoretical approximation DFT B3LYP/6-31G(d) can be used to inspect the molecular orbitals that contribute to the excitation process in organic molecules. This analysis was carried out only in the 2-2-2 and 3-3-3 3D-structures because these molecules presented the lowest energy gap and the best bathochromic displacement in the UV spectral analysis. The excitation properties and the feasibility of electron or hole transport are influenced strongly by the shapes of the frontier energetic levels. This examination as well as contour plots of HOMOs and LUMOs are shown in Tables 3 and 4 (isovalue=0.02). Based on the electronic transition analysis, we selected the highest occupied and the three lowest unoccupied molecular orbitals, denoted as HOMO, LUMO, LUMO+1 y LUMO+2, respectively. It can be seen that, for the 2-2-2 and 3-3-3 dendrimers, the HOMO orbital is localized mainly in the TPA core—this core being the electron-rich inner part of the molecule. Also, it is well known that the HOMO orbital can be an approximation of the electron donor capacity of any system, while the LUMO molecular orbital can be interpreted in a semiquantitative way as the electron acceptor capacity. The LUMO, LUMO+1 and LUMO+2 orbitals in the 3-3-3 molecule are localized in the three dendrons attached to the central core (see Table 4); these dendrons can act as the electron-deficient peripheral part of

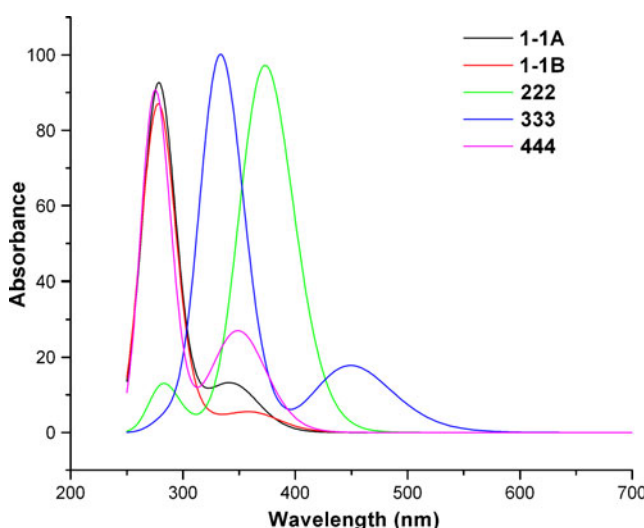


Fig. 4 Comparison of UV absorption spectra of pyrrolic derivatives calculated with time-dependent density functional theory (TD-DFT) B3LYP/6-31G(d)

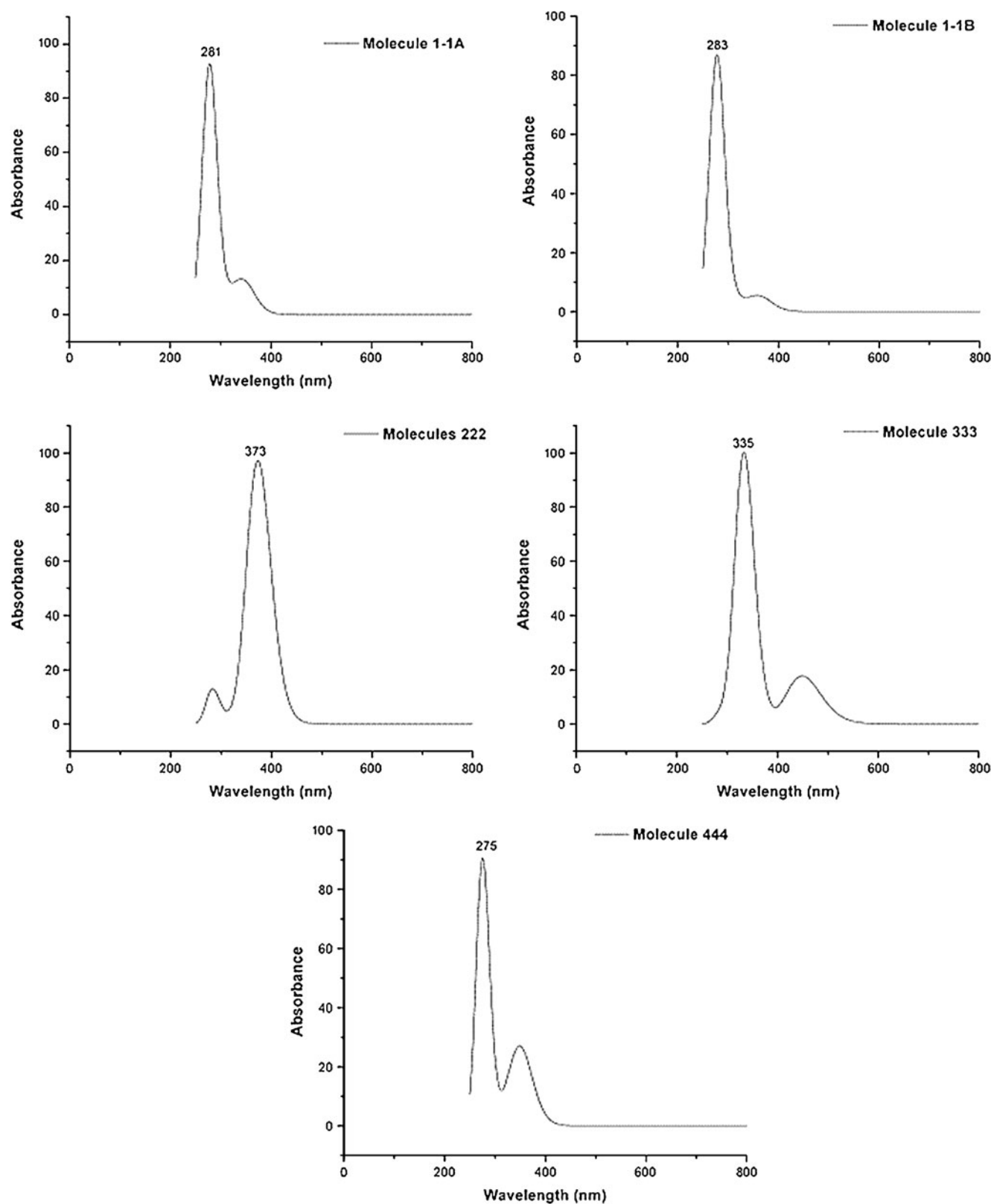
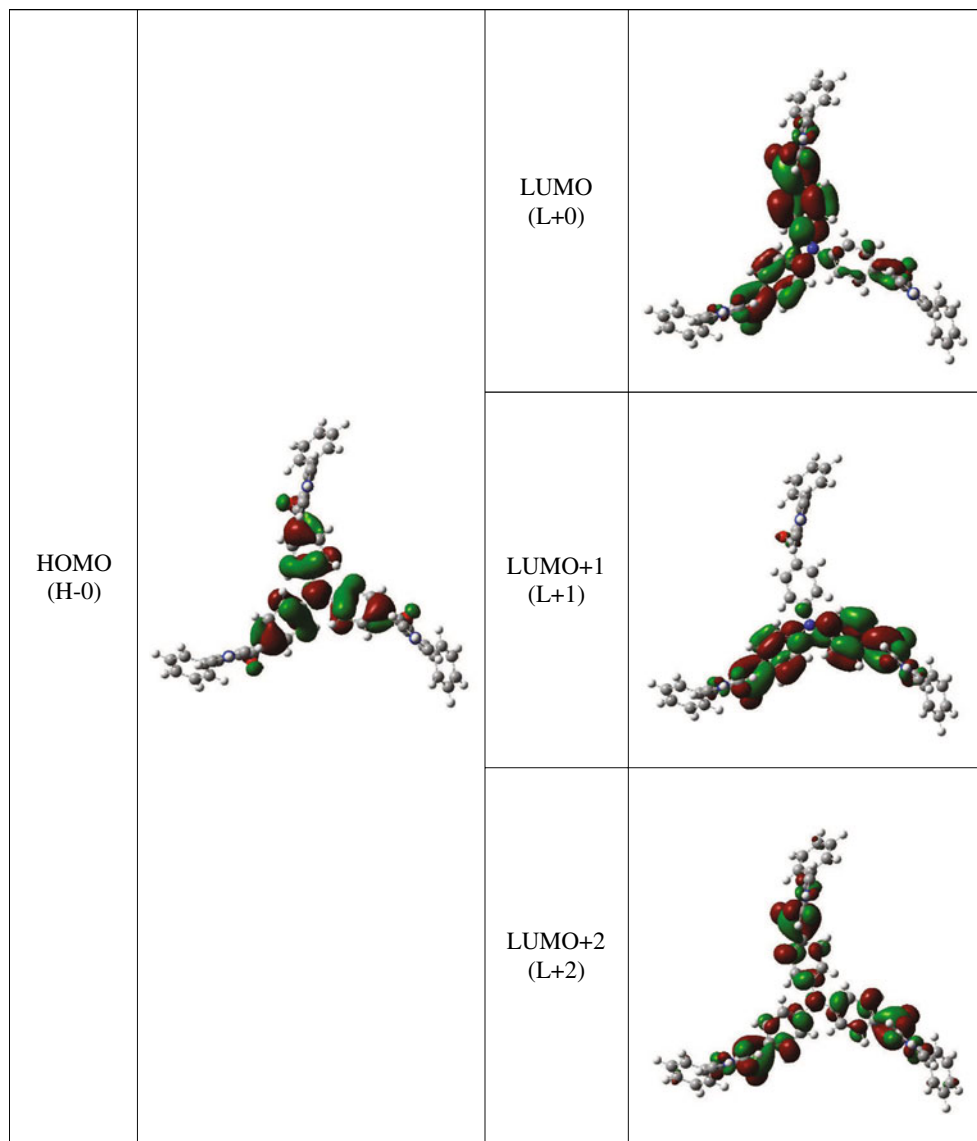


Fig. 5 Single absorption spectrum of the five proposed systems obtained with TD-DFT B3LYP/6-31G(d)

Table 3 Contour plots of HOMOs and LUMOs for molecule 2-2-2

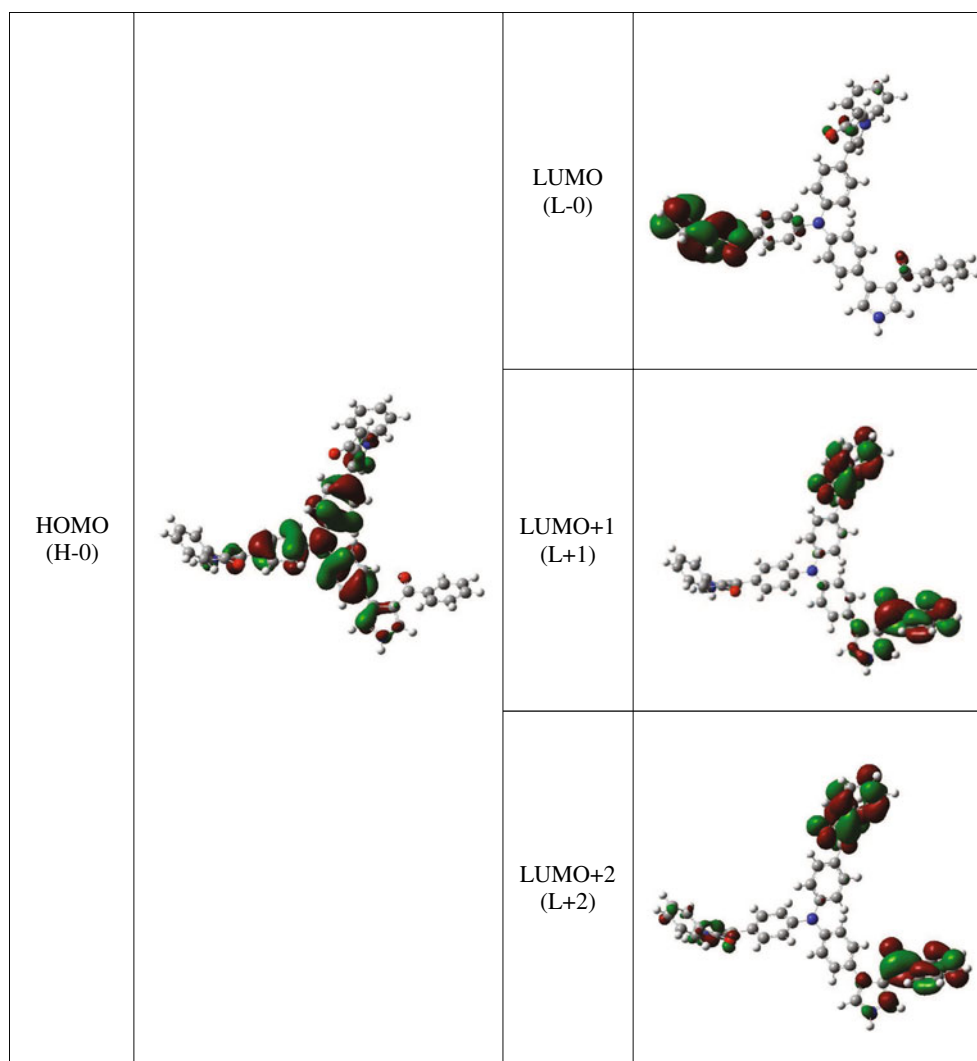
the molecule. As a first approximation, the ICT phenomenon reflects the intramolecular donor-acceptor interactions between the central and external zones of the same system. Other important donor-acceptor interactions can involve neighboring molecules (intermolecular charge transfer) [38].

Electronic transition analysis

Electronic transitions in the 2-2-2 and 3-3-3 dendrimers were analyzed in order to confirm the HOMO and LUMO localizations as well as the molecular orbital levels involving in donor-acceptor interactions. Electronic transition states, maximum absorption wavelength (λ_{\max}), vertical absorption energy (Ω_A) and oscillator strengths (f), calculated with TD-DFT and the B3LYP/6-31G(d) level of

theory for the most important singlet excited states in 2-2-2 and 3-3-3 molecules are listed in Tables 5 and 6, respectively.

The calculated properties revealed that the strongest electron transitions with largest oscillator strength correspond essentially to the promotion of an electron from HOMO to LUMO and nearby molecular orbitals. The 2-2-2 molecule presents two closer absorption bands with values of 373.85 and 373.61 nm, composed of HOMO (H-0) to LUMO (L+0) followed by HOMO (H-0) to LUMO+1 (L+1) orbital transitions, which have similar oscillator strength values, indicating almost the same intensity in the two bands. The vertical transition energies (Ω_A) obtained for this system were 3.31 eV for both bands. As expected, the analysis of subsequent electronic transitions presents

Table 4 Contour plots of HOMOs and LUMOs for molecule 3-3-3

smaller oscillator strengths involving internal molecular orbitals with largest vertical absorption energies. The relationship between the more intensive electronic transitions and the localization of HOMOs and LUMOs demonstrated that the donor and acceptor zones are situated in almost the same place in molecule 2-2-2 (see Table 5),

which could minimize the electronic transfer process in this dendrimer.

The second band of the absorption spectrum was analyzed for the 3-3-3 molecule. This band is nearest to the maximum of the terrestrial solar spectrum (see Fig. 4), and the electronic transitions presented in this system were

Table 5 Electronic transition states of molecule 2-2-2, maximum absorption wavelength (λ_{\max}), vertical absorption energy (Ω_A), oscillator strengths (f), and transition assignments as calculated with TD-DFT and the B3LYP/6-31G(d) level of theory

λ_{\max} (nm)	Ω_A (eV)	Oscillator strength (f)	Electronic transition
373.85	3.316	0.6153	$H-0 \rightarrow L+0$
			$H-0 \rightarrow L+1$
373.61	3.319	0.6162	$H-0 \rightarrow L+0$
			$H-0 \rightarrow L+1$

Table 6 Electronic transition states of molecule 3-3-3, λ_{\max} , Ω_A , (f), and transition assignments as calculated with TD-DFT and the B3LYP/6-31 G(d) level of theory

λ_{\max} (nm)	Ω_A (eV)	Oscillator strength (f)	Electronic transition
451.39	2.75	0.1073	$H-0 \rightarrow L+0$
			$H-0 \rightarrow L+2$
448.72	2.76	0.0652	$H-0 \rightarrow L+0$
			$H-0 \rightarrow L+1$
442.01	2.81	0.0245	$H-0 \rightarrow L+1$
			$H-0 \rightarrow L+2$

between neighboring orbitals: HOMO (H-0), LUMO (L-0), LUMO+1 (L+1) and LUMO+2 (L+2) with lowest vertical absorption energies in a range from 2.75 to 2.81 eV (see Table 6). From these calculations, it also becomes apparent that the localization of HOMOs and LUMOs, as well as the electronic transitions involved, clearly show that the central core TPA is the electron-rich, or electron donor, part of the molecule in which the HOMO orbital is localized. The external parts of dendrons present electron deficiency and the LUMO (L-0), LUMO+1 (L+1) and LUMO+2 (L+2) orbitals map in these acceptor zones. This characteristic could facilitate the intramolecular charge transfer, and the electronic flux practically fills the whole molecular structure.

Conclusions

Density functional theory and TD-DFT approaches were used to analyze five pyrrolic ring derivatives, with some of these derivatives presenting 3D conjugated architectures with a central core of TPA and π -conjugated rings attached to the core-formed dendrons. The electronic properties calculated in this study indicated that HOMO–LUMO gap energy for the 3D-system with the so-called 3-3-3 molecule exhibited the smallest value at 3.14 eV—a large reduction in gap energy was obtained for this system. Ultraviolet spectra obtained for each compound revealed a second band that can be attributed to ICT in some derivatives, with the 3-3-3 molecule presenting the band nearest to the solar spectrum range (500–800 nm). Analysis of the localization of HOMOs and LUMOs revealed that, in the structures denoted as 2-2-2 and 3-3-3 according to their 3D-architecture, the electron-rich or donor zone was localized in the central TPA core while the acceptor zone is indicated to be LUMOs, with these being contained mainly in the electron-deficient part of the molecule corresponding to the peripheral rings. This facilitates the ICT phenomenon, whereby the 2-2-2 and 3-3-3 dendrimers exhibit the best electronic and structural characteristics to be employed as organic semiconductor molecules. However, complete photophysical investigations into charge recombination and electron transport, and also the ICT processes involved in these systems, are required to confirm the theoretical results obtained in this work.

Acknowledgments This work is supported by Universidad Autónoma de Chihuahua (UACH), with financial support UACH-CA-086/2007. R. M.G.P. and L.M.R.V. acknowledges project. L.M.R.V. thanks the Facultad de Ciencias Químicas (FCQ). N.F.H. and D.G.M. thank CIMAV.

References

- Xue J, Rand BP, Uchida S, Forrest SR (2005) A hybrid planar-mixed molecular heterojunction photovoltaic cell. *Adv Mat* 17:66–71
- Mullen K, Scherf U (2006) Organic light emitting devices. Wiley, Weinheim
- Günes S, Neugebauer H, Sariciftci NS (2007) Conjugated polymer-based organic solar cells. *Chem Rev* 107:1324–1338
- Anthony JE (2006) Functionalized acenes and heteroacenes for organic electronics. *Chem Rev* 106:5028–5030
- Murphy AR, Frechet JM (2007) Organic semiconducting oligomers for use in thin film transistors. *J Chem Rev* 107:1778–1787
- Thomas SW III, Joly GD, Swager M (2007) Chemical sensors based on amplifying fluorescent conjugated polymers. *Chem Rev* 107:1339–1386
- Ren Y, Dienes Y, Hettel S, Parvez M, Hoge B, Baumgartner (2009) Highly fluorinated dithieno[3, 2-b:2', 3'-d] phospholes with stabilized LUMO levels. *T Organometallics* 28:734–740
- Archer M, Nozik AJ (2008) nanostructured and photoelectrochemical systems for solar photon conversion. Imperial College, London
- Çagin T, Wang G, Martin R, Breen N, Goddard W (2000) Molecular modeling of dendrimers for nanoscale applications. *Nanotechnology* 11:77–84
- Lo SC, Burn PL (2007) Development of dendrimers: macromolecules for use in organic light-emitting diodes and solar cells. *Chem Rev* 107:1097–1116
- Mitchell WJ, Ferguson AJ, Köse ME, Rupert L, Ginley DS, Rumbles G, Shaheen SE, Kopidakis N (2009) Structure-dependent photophysics of first-generation phenyl-cored thiophene dendrimers. *Chem Mater* 21:287–297
- Shirota YJ (2000) Photo and electroactive amorphous molecular materials design, synthesis, reactions, properties and applications. *J Mater Chem* 15:75–93
- Nishimura K, Kobata T, Inada H, Shirota Y (1991) Arylaldehyde and arylketone hydrazones as a new class of amorphous molecular materials. *J Mater Chem* 1:897–898
- Ohishi H, Tanaka M, Kegeyama H, Shirota Y (2004) Amorphous molecular materials with high carrier mobilities: thiophene and selenophene containing tris(oligoarylenyl) amines. *Chem Lett* 33:1266–1267
- Köse ME, Mitchell WJ, Kopidakis N, Chang CH, Shaheen SE, Kim K, Rumbles GJ (2007) Theoretical studies on conjugated phenyl-cored thiophene dendrimers for photovoltaic applications. *J Am Chem Soc* 129:14257–14270
- Supritz C, Engelmann A, Reineker P (2006) Energy transport in dendrimers. *J Lumin* 119:337–340
- Beenken WJD (2009) Photo-induced charge transfer in fullerene-oligothiophene dyads- A quantum –chemical study. *Chem Phys* 357:144–150
- Yang L, Feng JK, Ren AM (2006) Structural, electronic and optical properties of a series of oligofluorene-thiophene oligomers and polymers. *J Mol Struct THEOCHEM* 758:29–39
- Sánchez-Bojorge N, Flores-Holguín N, Glossman-Mitnik D, Rodríguez-Valdez LM (2009) Computational note on the chemical reactivity of pyrrole derivatives. *J Mol Struct THEOCHEM* 912:119–120
- Grimme S (2004) Calculation of the electronic spectra of large molecules. In: Lipkowitz KB, Larter R, Cundari TR (eds) *Reviews in computational chemistry*, vol 20. Wiley, Hoboken, NJ
- Stephens PJ, Devlin FJ, Chabalowski CF, Frisch MJ (1994) Ab Initio calculation of vibrational absorption and circular dichroism spectra using density functional force fields. *J Phys Chem* 98:11623–11627
- Becke AD (1993) Density-functional thermochemistry III. The role of exact exchange. *J Chem Phys* 98:5648–5647
- Lee C, Yang W, Parr RG (1988) Development of the Colle-Salvetti correlation-energy formula into a functional of the electron density. *Phys Rev B* 37:785–789

24. Petersson GA, Al-Laham MA (1991) A complete basis set model chemistry. II. Open-shell systems and the total energies of the first-row atoms. *J Chem Phys* 94:6081–6090
25. Sun M (2006) Excited state properties of novel p- and n-type organic semiconductors with an anthracene unit. *Chem Phys* 320:155–163
26. Sun M, Kjellberg P, Beenken WJD, Pullerits T (2006) Comparison of the electronic structure of PPV and its derivative DIOXA-PPV. *Chem Phys* 327:474–484
27. Hwan Park Y, Hee Rho H, Gill Park N, Sik Kim Y (2005) Theoretical investigation of tetra-substituted pyrenes for organic light emitting. *Curr Appl Phys* 6(4):691–694
28. Bartolotti L (1982) Time-dependent Kohn-Sham density-functional theory. *J Phys Rev A* 26:2243–2244
29. Runge E, Gross EKU (1984) Density-functional theory for time-dependent systems. *Phys Rev Lett* 52:997–1000
30. Casida ME (1995) In: Chong DP (ed) Recent advances in density functional methods, vol 1. World Scientific, Singapore
31. Frisch MJ (2003) GAUSSIAN03 Rev B.01. Gaussian Inc, Pittsburgh
32. Brüting W (2005) Physics of organic semiconductors. Wiley, Berlin
33. Requena A, Zuñiga J (2004) Espectroscopia. Pearson, Madrid
34. Davenas J, Ltaief A, Chaabane BR, Bouazizi A (2006) Photovoltaic properties of bulk heterojunction solar cells with improved spectral coverage. *Mater Sci Eng C* 26:344–347
35. Kymakis E, Amarantunga GAJ (2003) Photovoltaic cells based on dye-sensitization of single-wall carbon nanotubes in a polymer matrix. *Sol Energy Mater Sol Cells* 80:465–472
36. Hoppe H, Sariciftci NS (2004) Organic solar cells: an overview. *J Mater Res* 19:1924–1945
37. López-Martínez EI, Rodríguez-Valdez LM, Flores-Holguín N, Márquez-Lucero A, Glossman-Mitnik D (2009) Theoretical study of electronic properties of organic photovoltaic materials. *J Comput Chem* 30:1028–1037
38. Roquet S, Cravino A, Leriche P, Alévêque O, Frére P, Roncalli J (2006) Triphenylamine-thiylenevinylene hybrid systems with internal charge transfer as donor materials for heterojunction solar cells. *J Am Chem Soc* 128:3459–3466